Determination of anisotropic deformability parameters of tuff by a single triaxial test

Yota Togashi[1], M. Kikumoto[2], and K. Tani[3]

[1] Graduate School of Science and Engineering, Saitama University, 255, Shimo-okubo Sakura-ku, Saitama 338-8570, Japan.
[2] Yokohama National University, 79-5, Tokiwadai Hodogaya-ku, Yokohama 240-8501, Japan.
[3] Tokyo University of Marine Science and Technology, 4-5-7, Konan Minato-ku, Tokyo 108-8477, Japan.

ABSTRACT

A method of determining deformation anisotropy by a single triaxial test was proposed and a new triaxial testing apparatus including a new cap with a slider mechanism and low friction sheets was developed by the authors. In this study, anisotropic deformation properties of a tuff sampled in Utsunomiya, Japan, were investigated by this method. Strain responses of four specimens sampled to different orientation during triaxial compression were observed in detail. The values of anisotropic deformability parameters of the specimens evaluated on each specimen and demonstrated that the Young's moduli in the bedding orientation are 1.5- 3.9 times larger than that in perpendicular orientation.

Keywords: anisotropy; sedimentary rock; triaxial test; transversely isotropy; tuff

1 INTRODUCTION

Sedimentary rocks usually exhibit anisotropic deformation characteristics due to their sedimentary structure. It is important to accurately evaluate such deformation anisotropy for rational designs of rock structures, e.g., foundation and tunnel. Deformation anisotropy has conventionally been determined by numerous tests using many specimens sampled from several orientations (e.g. Oka et al., 2002). However, this is both costly and time consuming. In addition, the orientations of anisotropy cannot be determined by such tests because the dominant orientation of anisotropy may not include in the sampling orientations. Therefore, a method of determining anisotropy by smaller number of tests is strongly needed.

The deformation of anisotropic rock specimen during triaxial test become non-axisymmetrical to the loading axes, as shown in Fig. 1, due to non-coaxial relationships between stresses and strains of the rock. On the basis of the fact, we developed a method of determining the anisotropy by a single triaxial test via isotropic consolidation and axial compression of rock specimen (Togashi et al., 2017a). This method is implemented via measuring the non-axisymmetrical deformation. Then, to achieve uniform deformation of the specimen as shown in Fig.1 (a), a new testing apparatus including a new low friction cap with sliding mechanism was developed. The proposed method were verified by the tests using rhyolitic welded tuff (Togashi et al. (2017b)). Furthermore, a determination method of anisotropy utilizing the non-uniform responses was also developed as shown in Fig.1(b) (Togashi et al., 2018a).

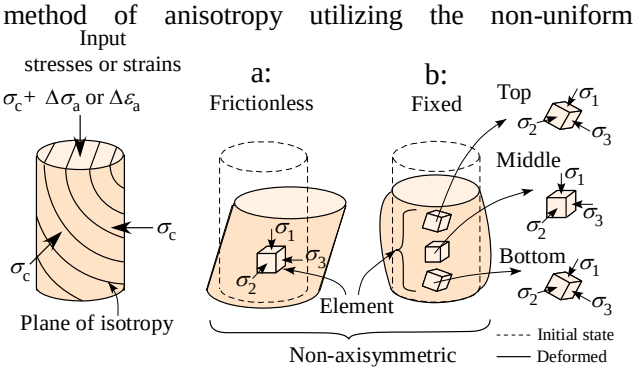

Fig.1 Non-axisymmetric deformation of anisotropic cylindrical specimen.

In this study, the results of four consolidated drained triaxial compression tests of the tuff specimen by the proposed method were shown and discussed. In addition to the results of previous study (Togashi et al. (2017b), Togashi et al. (2018b)), non-coaxial stress-strain relationships of the tuff due to bedding orientation are discussed by small strain tensor measurements. Then, anisotropic parameters of the sample are determined by the proposed method.

2 TEST METHOD

To obtain correct elementary responses of anisotropic rock sample, a cap with a sliding mechanism including Teflon sheets with lubricant was

developed as shown in Fig. 2 (Togashi et al. 2017b). The non-axisymmetric deformation of the specimen is consequently allowed as shown in Fig. 2 (b). Triaxial compression tests are conducted by using this cap.

Tage tuff, which is rhyolitic welded tuff of Neogene period, is sampled from a depth of 100 m in Utsunomiya, Japan. Four cylindrical specimens (diameter d = 50 mm and height h = 100 mm) were cored from a 30 cm cubic block, as shown in the test cases (Table 1). As the block has apparent bedding planes as shown in Fig. 3. The specimens were fully saturated before loading in accordance with the Japanese Geotechnical Standard (JGS, 2009). The variation in the wet densities of the specimens was very small at ρ_t = 1.72– 1.79 g / cm^3. Both ends of the specimens were shaped with parallelisms of less than 0.05 mm (JIS B 0621).

Consolidated-drained triaxial compression tests were conducted on four samples for which the bedding plane was inclined at 15°, 30°, 45° and – 45°, respectively. First, the specimens were isotropically consolidated with a mean effective stress σ'_c = 1.0 MPa (cell pressure σ_c = 1.2 MPa, back pressure u_b = 0.2 MPa), for the steady state of the strain was achieved. The specimens were then axially compressed. The axial strain rate during compression was set to 0.03% / min, as adopted by Oka et al. (2002).

To evaluate non-axisymmetric deformation of the specimen, nine normal small strains were measured using three rosette gauges attached on the lateral surface, as shown in Fig. 4. The six components of the small strain tensor $\boldsymbol{\varepsilon}$ in (X, Y, Z) coordinate are calculated using the least square method, based on the normal strains $\mathbf{x}$ measured by nine strain gauges as:

$$\boldsymbol{\varepsilon} = (\mathbf{E}^{\mathrm{T}}\mathbf{E})^{-1}\mathbf{E}^{\mathrm{T}}\mathbf{x} \qquad (1)$$

where $\mathbf{E}$ is a 9 × 6 matrix, as given by the unitary directional vectors of the nine strain gauges. The specific components of $\mathbf{E}$ is shown in the previous study (Togashi et al., 2017b).

3 RESULTS AND DISCUSSION

Table 2 lists measured strain tensors in the steady state after isotropic consolidation. The specimens exhibit clear anisotropy, because the *XX*, *YY*, and *ZZ* components of the strain tensors exhibit significantly different values and the shear strains (*XY*, *ZY*, and *ZX* components) were not zero. The values for the maximum, intermediate, and minimum principal strains listed in Table 3 all differ from each other.

Figure 5 shows the relationships between the axial stress increment and strain tensor increment during axial compression. The normal strain of axial orientation, $\Delta\varepsilon_{ZZ}$, is dominant during axial compression. Table 4 listed the tangential Young's moduli $E_{t,\,50}$ and the peak deviator stress $(\sigma_a - \sigma'_c)_{max} = \Delta\sigma_{a,max}$. The tests were confirmed as being reproducible because almost

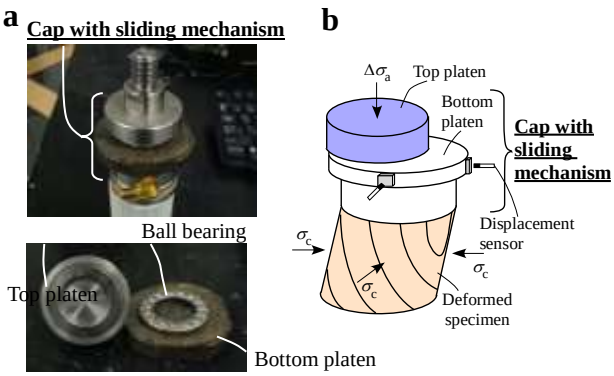

Fig.2 A cap with sliding mechanism. The structure and expected deformation are shown in (a) and (b) respectively.

Table 1 Test cases.

Case	Orientations of bedding plane ξ (°)	Wet density ρ_t (g/cm^3)	Cell pressure σ_c (MPa)	Back pressure u_b (MPa)	σ'_c (MPa)	Strain rate (% / min)
1	15	1.766	1.2	0.2	1.0	0.03
2	30	1.721				
3	45	1.740				
4	-45	1.756				

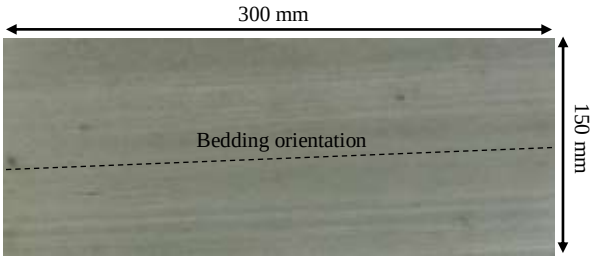

Fig. 3 Lateral surface of a Tage tuff block.

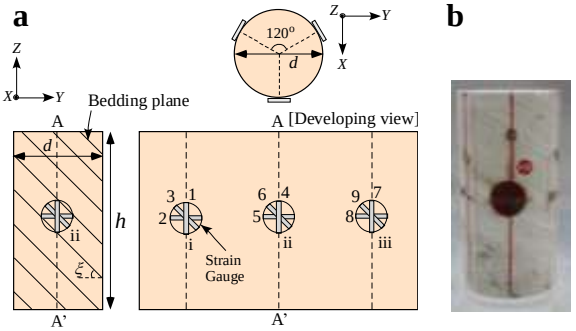

Fig. 4 A method of strain tensor measurement. (a) shows settings of rosette gauges and (b) is the condition of (ii) gauge.

Table 2 Strain tensor during isotropic consolidation.

ξ (°)	t (min)	σ'_c (MPa)	ε_{ij} (%) $(i, j = X, Y, Z)$					
			XX	YY	ZZ	XY	ZY	ZX
15	61	1.00	0.056	0.022	0.044	-0.004	0.005	0.002
30	61	1.00	0.040	0.066	0.041	-0.014	0.060	-0.028
45	132	1.00	-0.005	0.044	0.028	0.017	0.012	-0.004
-45	54	1.01	0.032	0.044	0.029	0.010	-0.016	0.005

Table 3 Principal strains during isotropic consolidation.

ξ (°)	t (min)	σ'_c (MPa)	ε_i (%) $(i = 1, 2, 3)$		
			1	2	3
15	61	1.00	0.051	0.046	0.006
30	61	1.00	0.125	0.034	-0.012
45	132	1.00	0.056	0.027	-0.019
-45	54	1.01	0.066	0.041	0.014

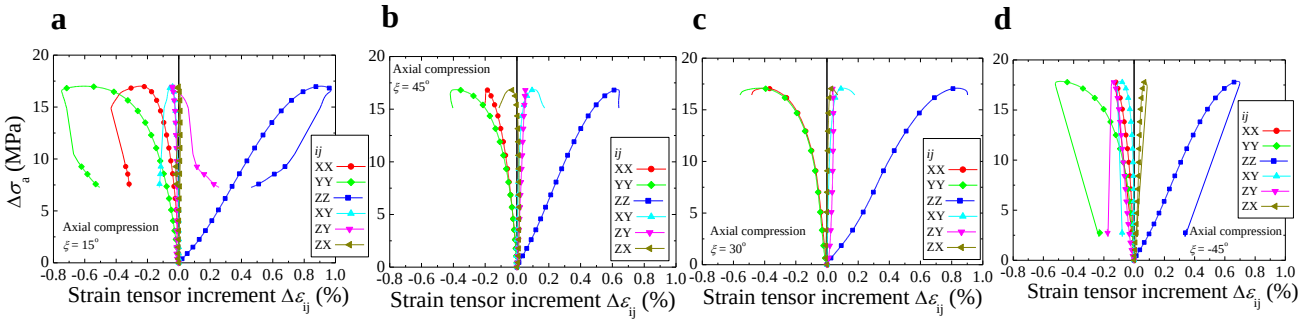

Fig.5 Strain tensor increments during axial compression ((a): ξ=15°, (b): ξ=30°, (c): ξ=45°, (d): ξ=-45°)

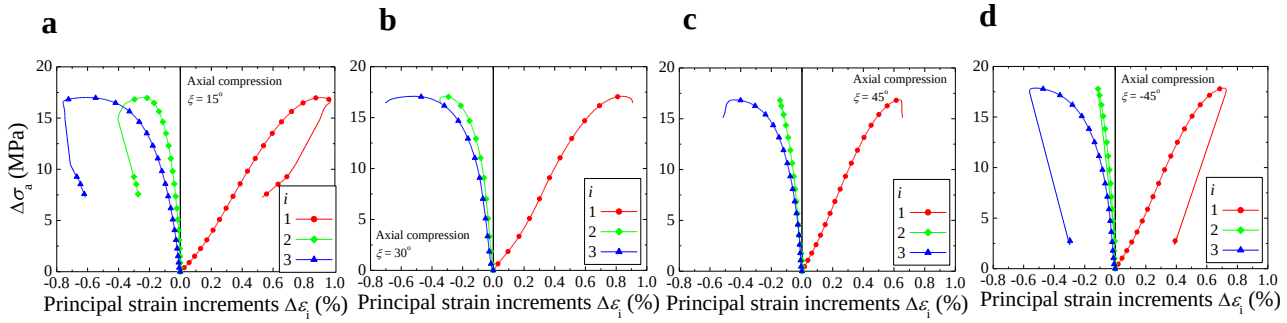

Fig.6 Principal strain increments during axial compression ((a): ξ=15°, (b): ξ=30°, (c): ξ=45°, (d): ξ=-45°)

the same values of $E_{t,50}$ and $\Delta\sigma_{a,max}$ are obtained in the symmetrical cases of ξ = 45° and - 45°. Figure 6 shows the relationships between the axial stress increment and the principal values of strain tensor increment.

Figure 7 shows the principal strain orientations in a steady state during isotropic compression by Ulf net of lower hemisphere projection (e.g. Shiono, 2008). The figure shows that the maximum principal strain ε_1 gets quite similar orientation to the bedding orientation in each case. It attributes the anisotropy of Tage tuff to the bedding plane.

The anisotropic stiffness and its dominant orientations of transversely isotropic elasticity (e.g. Pickering, 1970) were obtained in each triaxial test at half the peak stresses, $\Delta\sigma_a/\Delta\sigma_{a,max}$ = 0.5. In this study, the dominant orientations of anisotropy are determined by the orientation of the maximum principal strain during isotropic consolidation as listed in Table 5, because the orientations of the principal strains are theoretically agreed with the dominant orientations of anisotropy by Togashi et al. (2017a). The angle of rotation around maximum principal strain orientation is thus considered to be the dip angle of plane of isotropy, ξ*. Table 6 lists the anisotropic stiffness using Eq. (2) by Togashi et al. (2017a).

$$\mathbf{C} = \left(\mathbf{A}^{\mathrm{T}}\mathbf{A}\right)^{-1}\mathbf{A}^{\mathrm{T}}\mathbf{k} \qquad (2)$$

where **C**, **A** and **k** are stiffness vector, matrix of the anisotropy direction and the vector of stresses and strains respectively. The strains are rotated around Z axis by the strike of plane of isotropy, ζ*, and substituted in **k**. In every case, the Young's moduli in the bedding orientation are 1.5-3.9 times greater than in the perpendicular orientation. For the Poisson's ratio, although similar values are obtained for ν_z in the cases

Table 4 Young's moduli and the peak deviator stress

Case	ξ (°)	$E_{t,50}$ (MPa)	$(\sigma_a - \sigma')_{max} = \Delta\sigma_{a,max}$
1	15	2599	17.0
2	30	3183	17.1
3	45	3563	16.9
4	-45	3553	17.9

of ξ = 15°, 30° and 45°, and for ν_x in that of ξ = 15°, 30°. However, its value tended to vary to a greater degree than that of the stiffness, and ν_x in ξ = - 45° gets negative Poisson's ratio. A negative Poisson's ratio for transversely isotropic was theoretically confirmed by laminated materials (Herakovich, 1984), and it was actually observed for London clay (e.g., Gasparre et al., 2007). However, there are the possibility of a result of measurement errors and/or the heterogeneous nature of the sample. The series of the test using Tage tuff should be continued to clarify the phenomena.

4 CONCLUSION

In this study, four consolidated-drained triaxial compression tests were conducted on tuff specimens including clear bedding structure. Non-axisymmetric deformation behaviors of the specimen were evaluated and its anisotropy was determined by the new triaxial test which can give elementary responses to the rock specimen.

The measured results in the triaxial tests demonstrated that the orientations of principal strains during isotropic consolidation were inclined in

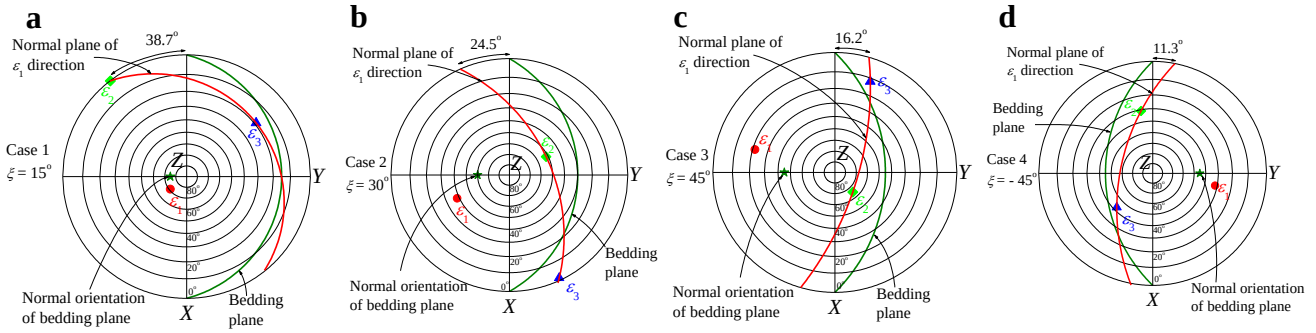

Fig.7 Relationships between the orientation of bedding plane and that of principal strain during isotropic consolidation by Ulf net. ((a): ξ=15°, (b): ξ=30°, (c): ξ=45°, (d): ξ=-45°)

accordance with the dip orientation of the bedding plane. The anisotropic elastic parameters were

Table 5 Directions of anisotropy. The orientation of plane of isotropy in transversely isotropic model was described by the rotation around symmetry axis ζ* and the inclination from the axis ξ*

Orientations of bedding plane ξ (°)	ζ* (°)	ξ* (°)
15	38.3	19.0
30	24.5	51.3
45	-16.3	68.6
-45	-11.3	-58.4

Table 6 Anisotropic elastic parameters of tuff

Orientations of bedding plane ξ (°)	E_z (MPa)	ν_z	G_z (MPa)	E_x (MPa)	ν_x
15	2048	0.046	896.1	3281	0.047
30	588.7	0.121	897.9	2277	0.022
45	1804	0.090	1130	3490	0.260
-45	959.8	0.207	1172	2597	-0.243

determined using both the proposed method and the ordinary method as the Young's moduli in the bedding orientation are 1.5–3.9 times larger than those in the perpendicular orientation.

ACKNOWLEDGEMENTS

We thank Mr. K. Ogawa and Mr. K. Hosoda at OYO corporation for their assistance with conducting triaxial tests.

REFERENCES

Japanese Geotechnical Society (JGS). (2009) Method for consolidated-drained triaxial compression test on rocks. JGS2534-2009.

Japanese Industrial Standards (JIS). (1984). Definitions and Designations of Geometrical Deviations. JIS B 0621-1984.

Gasparre A., Nishimura S., Minh N. A., Coop M. R., and Jardine R. J. (2007). The stiffness of natural London clay. Géotechnique. 57 (1), 33-47.

Herakovich C. T. (1984). Composite laminates with negative Poisson's ratios. Journal of Composite Materials. 18, 447-455.

Oka, F., Kimoto, S., Kobayashi, H., and Adachi, T. (2002). Anisotropic behavior of soft sedimentary rock. Soils and Foundations, 42(5), 59-70.

Pickering DJ. (1970). Anisotropic elastic parameters for soils, Géotechnique. 20(3), 271-276.

Shiono, S. (2008). Introduction to geometric vector for geologic mapping: numerical analysis of orientation data. Geoinformatics. 19(1), 13-46. (in Japanese)

Togashi, Y., Kikumoto M., and Tani K. (2017a). An experimental method to determine the elastic properties of transversely isotropic rocks by a single triaxial test. Rock Mechanics and Rock Engineering, 50(1), 1-15.

Togashi, Y., Kikumoto, M., Tani K., Hosoda, K. and Ogawa, K. (2017b) Determination and its verification of anisotropic stiffness of tuff by a single triaxial test, Japanese Geotechnical Journal. 12(1), 123-134. (in Japanese)

Togashi, Y., Kikumoto, M., and Tani. K. (2018a). Determining anisotropic elastic parameters of transversely isotropic rocks through single torsional shear test and theoretical analysis. Journal of Petroleum Science and Engineering, 169, 184-199.

Togashi, Y., Kikumoto, M., Tani, K., Hosoda, K. and Ogawa, K. (2018b). Detection of deformation anisotropy of tuff by a single triaxial test on a single specimen. International Journal of Rock Mechanics and Mining Sciences, 108, 23-36.